

Probing the High-Redshift Universe with Quasar Elemental Abundances

Fred Hamann

Center for Astrophysics & Space Sciences, University of California – San Diego, La Jolla, CA 92093-0424

Abstract. The heavy elements near QSOs provide unique measures of the star formation and chemical evolution in young galactic nuclei or pre-galactic condensations. Studies of quasar abundances also naturally address a variety of questions regarding the physics of QSO environments, including the Baldwin Effect emphasized at this meeting. Here I review the status of quasar abundance work.

1. Introduction

Quasars (or QSOs) at all redshifts have strong emission and (sometimes) absorption lines due to metals in their immediate environments. The gas must have undergone some amount of chemical enrichment, presumably via local star formation. At the highest quasar redshifts, approaching $z \sim 5$ (Schneider, Schmidt & Gunn 1991), the enrichment time scales cannot be long; the Universe itself was less than $(1+z)^{-1} \approx 17\%$ of its present age at $z = 5$, or roughly 1 billion years old (depending on the cosmology, see Fig. 1). Quasar metal abundances can therefore provide valuable constraints on the properties of star formation in the early Universe, possibly for the first stars forming in young galactic nuclei or pre-galactic condensations. These constraints will be important complements to other studies of high-redshift galaxies, involving, for example, the “Lyman-break” objects (Steidel *et al.* 1998, Connolly *et al.* 1997) or damped-Ly α absorbers (Pettini *et al.* 1997, Lu, Sargent & Barlow 1998), that probe more extended structures or rely on very different data and analysis techniques. An important goal of quasar research is therefore to merge the QSO abundance results with these other studies to develop a more complete picture of star formation and galaxy evolution at early cosmological epochs.

Quasar abundance studies also naturally address a variety of problems concerning the QSOs themselves, such as the circumstances of QSO formation and evolution, the location, geometry, dynamics and physical conditions of the emission and absorption line regions, the relationships between the various emission and absorption phenomena (including the soft X-ray “warm” absorbers), and the influence of metallicity on the physics and observable properties of QSO environments. The last of these items specifically involves the Baldwin Effect (see Osmer & Shields and Korista *et al.* in this volume).

Three independent probes of QSO abundances are readily observable at all redshifts: the broad emission lines (BELs), the broad absorption lines (BALs) and the intrinsic narrow absorption lines (NALs). Each diagnostic has its own

theoretical and observational uncertainties, so it is important to consider as many of them as possible. Here I review the status of QSO abundance studies based on these diagnostics. I will emphasize my own ongoing work with various collaborators. Please see Hamann & Ferland (1999 – hereafter HF99) for a more thorough review of this topic.

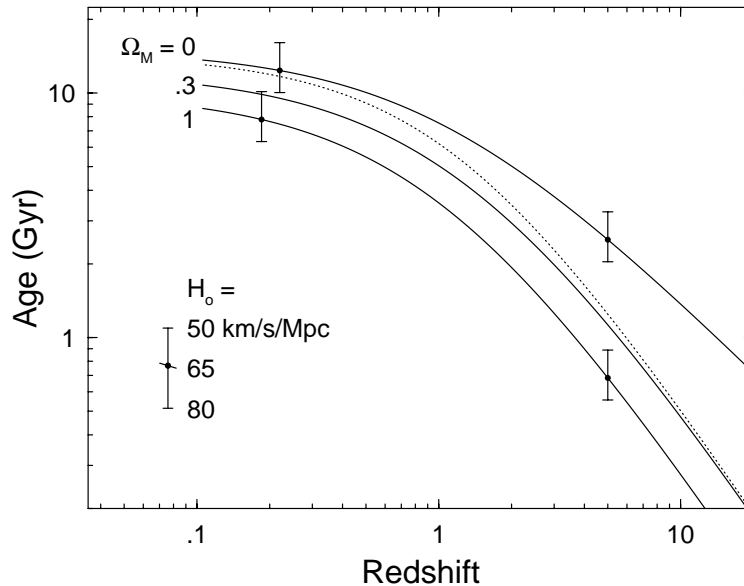


Figure 1. Redshift versus age of the Universe in Big Bang cosmologies. The three solid curves correspond to $H_o = 65 \text{ km s}^{-1} \text{ Mpc}^{-1}$, $\Omega_\Lambda = 0$ and $\Omega_M = 0, 0.3$ and 1 . The dotted curve corresponds to $\Omega_\Lambda = 0.7$ and $\Omega_M = 0.3$. The “error” bars show the range of ages possible for H_o between 50 and $80 \text{ km s}^{-1} \text{ Mpc}^{-1}$ (see Carroll & Press 1992).

2. Quasars and Galaxy Evolution

QSOs are believed to reside in the cores of massive galaxies or, perhaps at the highest redshifts, in dense condensations that later become the cores of massive galaxies. See, for example, Kormendy *et al.* (1998), Magorrian *et al.* (1998) for the black hole–host galaxy connection, McLure *et al.* (1998), McLeod (1998), Aretxaga, Terlevich & Boyle (1998), Bahcall *et al.* (1997), Miller, Tran & Sheinis (1996), McLeod & Rieke (1995) for direct observations of QSO hosts, and Turner (1991), Haehnelt & Rees (1993), Loeb & Rasio (1994), Haehnelt, Natarajan & Rees (1998), Haiman & Loeb (1998) for theoretical links between QSOs and galaxy formation.

2.1. Expectations for QSO Abundances

The intrinsic emission and absorption lines of QSOs offer direct probes of the composition and enrichment history of the gas in these dense galactic environments. Studies of nearby galaxies indicate that vigorous star formation

in galactic cores should have produced super-solar gas-phase metallicities (Z) within a few billion years of the initial collapse (e.g. Arimoto & Yoshii 1987; Köppen & Arimoto 1990). The enriched gas might ultimately be ejected from the galaxy/QSO environment, consumed by the central black hole, or diluted by subsequent gaseous infall, but the evidence for early-epoch high- Z gas remains in the old stars today. In particular, the mean stellar metallicities¹ in the cores of nearby massive galaxies (including the bulge of our own Milky Way) are typically ~ 1 to $3 Z_{\odot}$ (e.g. Rich 1988, Bica, Arimoto & Alloin 1988, Bica, Alloin & Schmidt 1990, Gorgas, Efsthathiou & Aragón Salamanca 1990, Worthey, Faber & Jesús Gonzalez 1992, McWilliam & Rich 1994, Minniti *et al.* 1995, Idiart *et al.* 1996, Bruzual *et al.* 1997). Individual stars are distributed about these means with metallicities reflecting the gas-phase abundance at the time of their formation. Only the most recently formed stars at any epoch have metallicities as high as that in the gas. Simple chemical evolution models of spheroidal systems like elliptical galaxies or the bulges spiral disks, wherein the gas-phase metallicity grows monotonically with time (Searle & Zinn 1978, Tinsley 1980, Rich 1990), predict that the gas was ~ 2 to 3 times more metal-rich than the current stellar means, or ~ 2 to $9 Z_{\odot}$ near the end of the main star-forming epoch. We might therefore expect QSO metallicities up to $\sim 9 Z_{\odot}$ as long as most of the local star formation (and enrichment) occurs before the QSOs “turn on” or become observable.

2.2. The Galactic Mass-Metallicity Relation

Studies of nearby galaxies reveal that higher metallicities occur in more massive systems (Faber 1973, Bender, Burstein & Faber 1993, Zaritsky, Kennicutt & Huchra 1994). Massive galaxies reach higher Z 's because they have deeper gravitational potentials and are better able to retain their gas against the building thermal pressures from supernovae (Larson 1974). Low-mass galaxies eject their gas before high Z 's are attained. Quasar abundance estimates should therefore constrain the gravitational binding energy of the local star-forming regions and, perhaps, the total masses of the host galaxies.

2.3. Fe/ α as a Cosmological Clock

Another relevant result from galactic chemical evolution is that the ratio of Fe to α -element (O, Ne, Mg, ...) abundances can constrain the ages of star-forming systems (Wheeler, Sneden & Truran 1989). The Fe/ α age constraint follows from the different enrichment timescales; α elements come from the supernova explosions of short-lived massive stars (primarily Type II – SN II's), while Fe has a large contribution from the longer-lived intermediate-mass binaries that produce Type Ia supernovae (SN Ia's). The subsequent delay in the Fe enrichment, roughly 1 Gyr, does not depend on the star formation rate or other uncertain parameters of the chemical evolution; it depends only on the lifetimes of the SN Ia precursors (see §3 below, also Yoshii, Tsujimoto & Nomoto 1996). The ratio of Fe/ α abundances can therefore serve as an absolute “clock” for constraining

¹Note that “metallicity” is measured best from the enrichment products of massive stars like O, Mg, etc., rather than Fe (see Wheeler *et al.* 1989 and §2.3 below).

the epoch of first star formation and, perhaps, the cosmology itself (see Hamann & Ferland 1993a – hereafter HF93a). For example, measurements of high Fe/α (near solar or higher) in $z > 4$ QSOs would place the epoch of star formation beyond the limits of current direct observations ($z > 6$) and might be problematic for cosmologies with $\Omega_M = 1$ (Fig. 1).

2.4. Nitrogen Abundances

A final result from galactic abundance studies is that nitrogen can also be selectively enhanced at moderate to high metallicities due to “secondary” CNO nucleosynthesis. There is growing evidence for a substantial “primary” N contribution at low Z in some objects, based on a plateau in $[\text{N}/\text{O}]$ at roughly -0.7 for $[\text{O}/\text{H}] \lesssim -0.7$ in galactic HII regions². But at higher metallicities (in the regime relevant to QSOs, see below), secondary production dominates and $[\text{N}/\text{O}]$ grows roughly in proportion to $[\text{O}/\text{H}]$ (HF93a, Vila-Costas & Edmunds 1993, Van Zee *et al.* 1998, Izotov & Thuan 1999). Shields (1976) noted that this special behavior should make nitrogen a particularly valuable probe of the chemical evolution in QSOs.

3. Specific Predictions for Galactic Chemical Evolution

Chemical enrichment models make specific predictions for the gas-phase abundances that can be compared to the QSO data. Hamann & Ferland 1992 and HF93a constructed one-zone models for stellar populations assembled by the infall of primordial gas. The enrichment follows standard stellar yields that compare well with observations of the Milky Way and nearby galaxies. The star formation is regulated by power-law initial mass functions (IMFs) of the form $\Phi \propto M^{-x}$, where M is the stellar mass and $\int \Phi \, dM = 1$. The enrichment delays caused by finite stellar lifetimes are included. We tested the calculations by constructing a simple yet viable model of the Galactic solar neighborhood, and then varied just the slope of the IMF and the timescales for star formation and infall to model the chemical history of QSO environments.

Figure 2 shows the predicted relative abundances for two cases at opposite extremes. The “Solar Neighborhood” model uses a 3 Gyr timescale for the infall of primordial gas and an IMF with slope $x = 1.6$ for $M \geq 1 M_\odot$ and 1.1 for $M < 1 M_\odot$ (after Scalo 1990). The stellar birth rate is set so that $Z = 1 Z_\odot$ at the time of the sun’s formation and the fraction of mass in gas is $\sim 15\%$ at the present epoch. The “Giant Elliptical” model uses a stellar birth-rate $\gtrsim 100$ times faster and an infall timescale of only 0.05 Gyr so that the mass fraction in gas is $\sim 15\%$ after just 0.5 Gyr. The IMF is also flatter, with slope $x = 1.1$ for all masses. The shorter timescales and flatter IMF (more high-mass stars) in the Giant Elliptical case produces a rapid evolution to high Z ’s, reaching $\sim 10 Z_\odot$ at ~ 1 Gyr. The star formation stops at ~ 1 Gyr because the gas is essentially exhausted; thereafter the system evolves “passively” and the ejecta from low-mass stars affect the abundances somewhat. See HF93a for details.

²I use the notation for logarithmic abundances relative to solar, $[a/b] = \log(a/b) - \log(b/a)_\odot$

The parameters used in these calculations were based on standard one-zone infall models of the Galactic disk and massive ellipticals (Arimoto & Yoshii 1987, Matteucci & Tornambé 1987, Matteucci & Brocato 1990, Köppen & Arimoto 1990). However, the results are only illustrative and more sophisticated models would be needed to match entire galaxies.

Both models in Figure 2 exhibit the delayed rise and subsequent overabundances in N (due to secondary CNO processing in stellar envelopes) and Fe (due to the delayed enrichment by Type Ia supernova). The late increase in Fe/α should be at least a factor of a few. The increase is larger in the Giant Elliptical case because, by the time SN Ia's make their Fe contribution, there is little gas left in the systems and each SN has a greater affect.

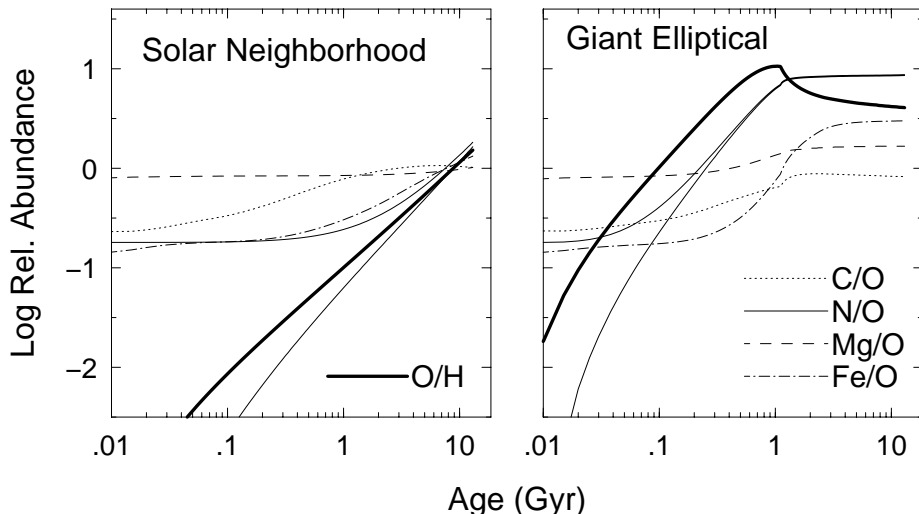


Figure 2. Logarithmic abundance ratios normalized to solar for the two evolution models discussed in the text. Two scenarios for the N enrichment are shown; one with secondary only and the other with secondary+primary (with a plateau in N/O at low Z that is forced to fit the HII region data; see §2.4).

4. Broad Emission Line Diagnostics and Results

Broad emission lines provide the most readily available abundance diagnostics because they are present in all QSOs. Many BELs can be measured in large QSO samples using medium-resolution spectra. However, the strengths of the metal lines, such as CIV $\lambda 1549$, relative to $\text{Ly}\alpha$ are surprisingly insensitive to the global metallicity (HF99, Hamann & Ferland 1993b). QSOs could actually have a very wide range of metallicities while displaying qualitatively similar BEL spectra (also Korista *et al.* 1998). Nonetheless, some line ratios are sensitive to the relative abundances. The challenge is to identify observable lines that have significant abundance sensitivities above their unavoidable dependences on other factors. In general, we must rely computational models to quantify the various parameter sensitivities. Since the BEL region (BELR) spans a range

of radii (Peterson 1993) and probably has a wide range of densities and ionizations (Ferland *et al.* 1992, Baldwin *et al.* 1995, Hamann *et al.* 1998), the most important criterion for abundance-sensitive line ratios is that they form under similar conditions (e.g. in the same or overlapping regions). Line ratios involving nitrogen should be particularly useful for constraining the total metallicity and evolutionary state of QSO environments (§2.4). Boyle (1990), Laor *et al.* (1995) and Osmer & Shields (this volume) present labeled plots showing the UV emission lines that are generally available for abundance studies.

4.1. Inter-combination Lines

Shields (1976, also Baldwin & Netzer 1978, Davidson & Netzer 1979, Osmer 1980, Uomoto 1984) used several ratios involving UV inter-combination (semi-forbidden) lines, such as NIII] λ 1750/CIII] λ 1909, NIII]/OIII] λ 1664 and NIV] λ 1486/CIV], to study the relative nitrogen abundances. The lines are often weak and difficult to measure, but these studies generally concluded that N/O and N/C are roughly solar or higher – consistent with solar or higher overall metallicities. That work fell out of favor by the mid-1980s as it became clear that BELR densities probably exceed the critical densities of the inter-combination lines ($\sim 3 \times 10^9$ to $\sim 10^{11}$ cm $^{-3}$). Thus collisional deexcitation, which was not previously accounted for, can be important. K.T Korista, G.J. Ferland and I have just begun a theoretical study to reexamine the usefulness of these ratios for abundance work. We suspect that at least some of the ratios (e.g. NIII]/OIII]) will prove to be useful abundance measures because the lines have similar critical densities and the collisional effects should roughly cancel out.

4.2. Ratios Involving NV λ 1240

Some early studies of the permitted BELs noted that NV λ 1240 was significantly stronger than the predictions of photoionization models (Osmer & Smith 1976, 1977). They noted that this NV enhancement might be due to a nitrogen enhancement as discussed by Shields (1976, §4.1). More recently, HF93a, Ferland *et al.* (1996) and Hamann *et al.* (1997a) performed extensive analysis of the NV λ 1240 emission compared to CIV λ 1549 and HeII λ 1640 for estimating N/He and N/C abundances. The NV/CIV line ratio is advantageous in low signal-to-noise spectra because CIV is essentially always present. The disadvantage of this ratio is that the NV and CIV line-forming regions are not quite coincident. The NV/HeII ratio can be harder to measure because HeII is weak, but upper limits on HeII still provide useful lower limits on the N/He abundance. NV/HeII is a more robust abundance indicator because the NV emitting region lies within the He $^{++}$ zone, where HeII λ 1640 forms by recombination. If N $^{+4}$ does not fill the He $^{++}$ zone the NV emission can be weak, but it is not possible to produce NV without also producing HeII (see also HF99 for more discussion).

We studied the theoretical NV/HeII and NV/CIV ratios for a wide variety of ionizing continuum shapes and BELR parameters. We used parameters that maximize (or nearly maximize) these ratios for comparisons to the data, so that we are most likely to underestimate the N/He and N/C abundances and thus the overall metallicity. Figure 3 compares the theoretical predictions to line ratios measured in QSOs at different redshifts. The predictions use abundances from Figure 2, a BELR density of 10^{10} cm $^{-3}$, an incident flux of hydrogen-ionizing

photons of $10^{20} \text{ cm}^{-2} \text{ s}^{-1}$, and the QSO continuum derived by Mathews and Ferland (1987; which we altered slightly to have $\alpha_{ox} = -1.24$ and an additional decline at wavelengths $\gtrsim 1 \mu\text{m}$). This continuum shape produces large but not quite maximum NV line ratios. See HF93a, Ferland *et al.* (1996) and Hamann *et al.* (1997a) for details on the calculations and the data set. The evolutionary ages from Figure 2 are converted to redshifts assuming the evolution begins at the Big Bang in a cosmology with $\Omega_M = 1$, $\Omega_\Lambda = 0$ and $H_o = 65 \text{ km s}^{-1} \text{ Mpc}^{-1}$. The results in Figure 3 show that the short timescales, flatter IMF (favoring high-mass stars) and higher Z 's in the Giant Elliptical model provide a much better fit to the high-redshift data. Steeper IMFs (more like the Solar Neighborhood case) could account for some of the smaller line ratios if the evolution times are short enough. The largest line ratios at high redshifts could be fit by invoking BELR parameters that better optimize the NV emission or by using still-flatter IMFs.

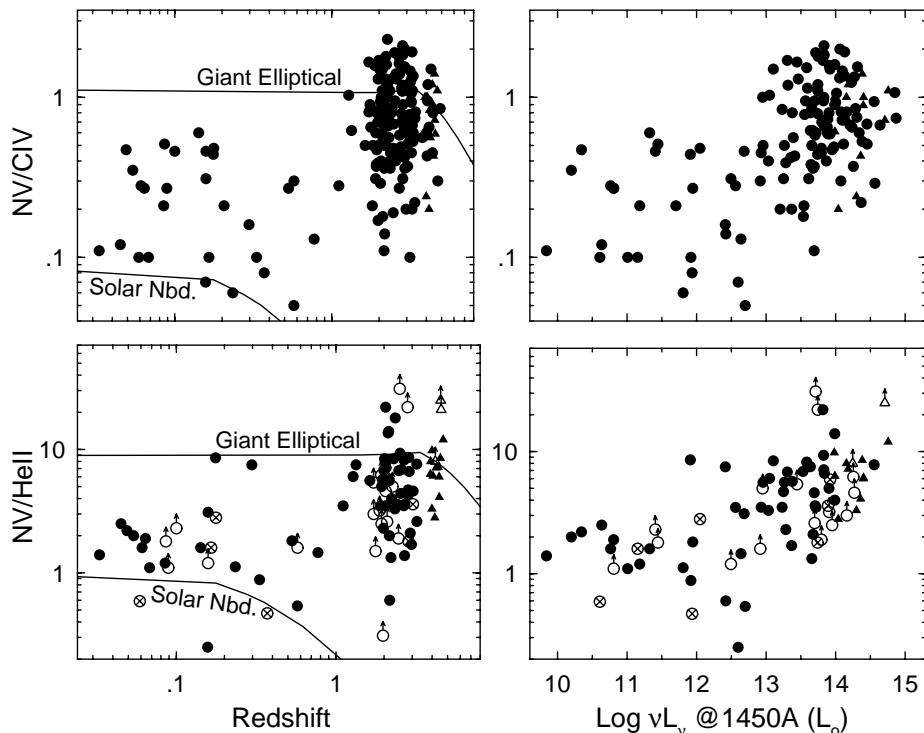


Figure 3. Observed and predicted NV/CIV and NV/HeII line ratios versus redshift (left panels) and luminosity (right panels) for a cosmology with $\Omega_M = 1$, $\Omega_\Lambda = 0$ and $H_o = 65 \text{ km s}^{-1} \text{ Mpc}^{-1}$ (see HF99).

One important empirical result is that the NV line ratios are typically larger in more luminous QSOs (HF93a, Osmer *et al.* 1994, Laor *et al.* 1995, Véron-Cetty, Véron, & Tarengi 1983). This trend could be affected by relationships between the luminosity L and various physical parameters of the BELR; however, the trend in the NV line ratios could also result entirely from higher metallicities (and higher relative N abundances) in more luminous sources (also Korišta *et al.* 1998 and this volume). If QSO luminosities correlate positively

with the masses of the QSOs and/or their host galaxies (McLeod & Rieke 1995, Magorrian *et al.* 1998), a metallicity- L relationship would indicate that there is a mass-metallicity relation among QSOs that is similar (or identical) to the well known relation in nearby galaxies (§2.2). The fact that high Z 's occur only at high redshifts (Fig. 3) might result from the natural tendency to form denser or more massive systems at early epochs, when the mean density of the Universe was itself higher (Haehnelt & Rees 1993).

4.3. Tests and Uncertainties

It should soon be possible to test the results based on NV for some QSOs using either the intercombination lines or other permitted line ratios such as NIII $\lambda 990$ /CIII $\lambda 977$ (Hamann, Korista & Ferland 1999). However, the main conclusion for $Z \gtrsim Z_{\odot}$ inferred from NV appears to be robust. It is not, for example, sensitive to uncertain parameters used in the photoionization calculations. In fact, adopting other (less than optimal) parameters only strengthens the case for large Z 's (Ferland *et al.* 1996). Photoionized gas is simply too cool to produce the large observed NV/HeII ratios with solar or lower N/He abundances. We therefore considered non-radiatively heated clouds, where higher temperatures might enhance the collisionally-excited NV line relative to the HeII recombination transition. We found that collisionally ionized clouds can indeed match the high NV/HeII ratios with roughly solar abundances if the temperatures are above 10^5 K. However, this situation still underpredicts the NV/CIV ratio – because both lines are collisionally excited – and overpredicts several other lines (e.g. SiIV $\lambda 1397$ and OIV] $\lambda 1402$). Such clouds are also thermally unstable and would tend to runaway to coronal temperatures (where no NV would be present) on thermal timescales of order tens of seconds (Hamann *et al.* 1995a, Ferland *et al.* 1996). Finally, we also explored the possibility that the NV emission is enhanced by scattering in an outflowing BAL region rather than by abundance effects (Krolik & Voit 1998, Turnshek *et al.* 1996, Turnshek 1988). Explicit calculations, which use observed BAL profiles for input and include scattering of both the underlying continuum and Ly α line radiation, indicate that the flux scattered by NV in BAL winds should contribute negligibly to the measured NV emission lines (Hamann & Korista 1996, Hamann *et al.* 1999, HF99).

4.4. FeII/MgII and Cosmology

The observed ratios of MgII $\lambda 2800$ to FeII (UV) emission lines might provide the Fe/ α age discriminator discussed in §2.3. The FeII emission spectrum is rich and blended, and the emission characteristics are not well understood because the Fe $^+$ atom is complex. Nonetheless, it is worth investigating because of the potential importance of Fe/ α abundances. FeII/MgII appears to be the best available emission-line diagnostic of Fe/ α because these lines have similar wavelengths and they should form in similar regions. They are also measurable in significant numbers of QSOs. Previous work on FeII (Wills, Netzer & Wills 1985) suggested that the Fe/Mg abundance ratio is typically several times larger than solar in QSOs (at moderate redshifts), indicating that the star formation began at least ~ 1 Gyr prior to the look-back times of those objects. More recent observations indicate that the FeII/MgII line ratios are large, consistent with

large Fe/Mg abundances, even in the highest redshift QSOs (at $z > 4$, Thompson, Elston & Hill 1999, Taniguchi *et al.* 1997). New theoretical calculations (Verner *et al.* 1999, Sigut & Pradhan 1998) of the FeII emission from BELRs will further test and quantify the FeII/MgII emission lines for abundance purposes.

5. Absorption Line Diagnostics and Results

5.1. Types of Absorption Lines

Intrinsic absorption lines provide independent probes of the elemental abundances near QSOs that can test and extend the emission-line results. Intrinsic absorbers include the BALs, at least some of the “associated” NALs (with similar absorption and emission redshifts, i.e. $z_a \approx z_e$), and any other systems that form in (or were ejected from) the vicinity of the QSO engine. Figures 4 and 5 show examples of QSO spectra containing BALs and NALs, respectively. BALs, with their broad troughs and maximum velocity extents often exceed-

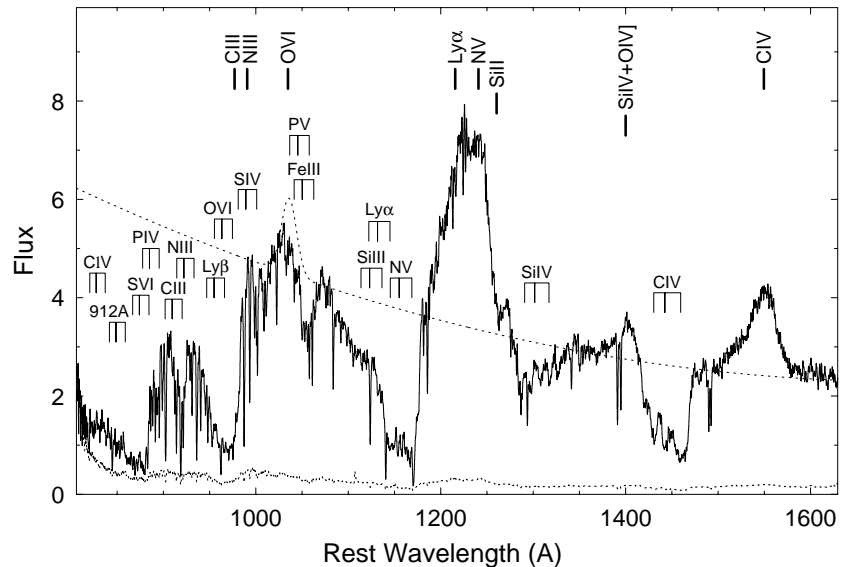


Figure 4. Spectrum of the BALQSO PG 1254+047 ($z_e = 1.01$) with emission lines labeled across the top and possible BALs marked at redshifts corresponding to the 3 deepest minima in CIV. Not all of the labeled BALs are present. The smooth dotted curve is a continuum fit extrapolated to short wavelengths (from Hamann 1998).

ing $10,000 \text{ km s}^{-1}$, clearly form in high-velocity outflows from the QSOs. NALs might form in a variety of environments, ranging from QSO winds like the BALs to cosmologically intervening gas like galactic halos. Each narrow-line system must be examined individually. Several indicators of intrinsic absorption have been developed, including (1) time-variable line strengths, (2) line multiplet ratios that imply partial line-of-sight coverage of the background light source(s), (3) high space densities inferred from excited-state fine-structure lines, and (4)

line profiles that are broad and smooth compared to thermal line widths (see Hamann *et al.* 1997b, Barlow & Sargent 1997 and references therein).

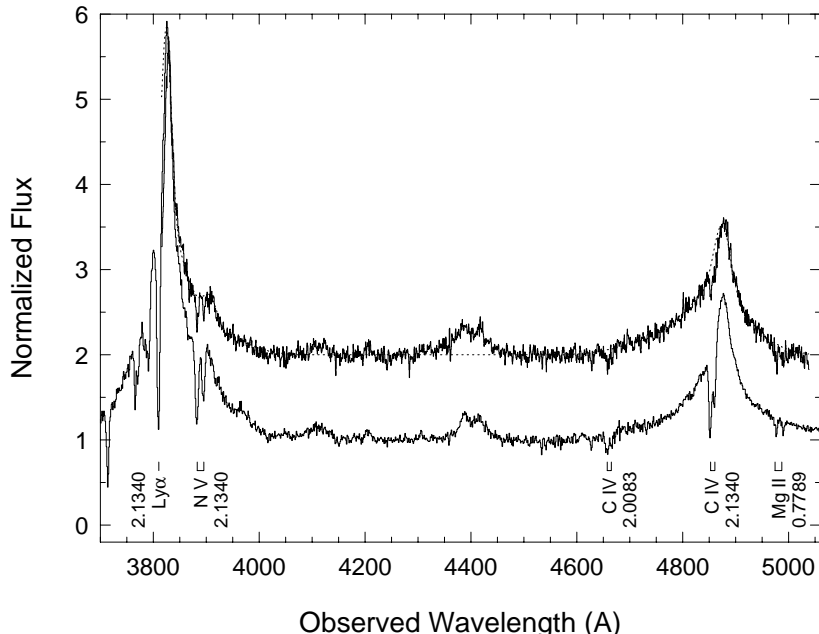


Figure 5. Normalized spectra of the QSO UM 675 ($z_e \approx 2.15$) show that its $z_a \approx z_e$ absorption lines (at $z_a = 2.134$) varied between two observations. The time variability, together with the relatively broad line profiles and partial line-of-sight coverage revealed by other higher-resolution data, imply that this NAL system is intrinsic to the QSO.

One well-studied example of an intrinsic narrow-line system is in the QSO, UM 675 (Hamann *et al.* 1995b, 1997b). Figure 5 shows that this system varied between two observations. At higher spectral resolution ($\sim 9 \text{ km s}^{-1}$) the line profiles appear much broader than the thermal speeds (with full widths at half minimum of $\sim 470 \text{ km s}^{-1}$) and the resolved CIV and NV line troughs appear too shallow for the optical depths required by their doublet ratios. The troughs are evidently filled-in by unabsorbed flux. This filling-in probably results from partial coverage of the background light source(s) (see HF99 for a sketch of possible partial-coverage geometries). The coverage fractions in UM 675 are $\sim 50\%$ for CIV and NV and $>85\%$ for HI. The variability time scale implies that the absorber is not more than 1 kpc from the central continuum source, and very likely much nearer. The diverse absorption lines detected in UM 675 (from CIII $\lambda 977$ and NIII $\lambda 990$ to OVI $\lambda 1034$ and NeVIII $\lambda 774$) imply a range of ionization states, consistent with a factor of $\gtrsim 100$ range in density or $\gtrsim 10$ in distance from the ionizing continuum source (see Hamann *et al.* 1997b).

5.2. General Techniques

The abundance analysis for absorption lines is, in principle, much simpler than for the emission lines because the absorption yields direct estimates of the ionic column densities. One only has to apply an ionization correction to convert

the column density ratios into relative abundances. The logarithmic abundance ratio of any two elements a and b is related to their column densities by,

$$\left[\frac{a}{b}\right] = \log\left(\frac{N(a_i)}{N(b_j)}\right) + \log\left(\frac{f(b_j)}{f(a_i)}\right) + \log\left(\frac{b}{a}\right)_\odot \quad (1)$$

where $(b/a)_\odot$ is the solar abundance ratio, and N and f are respectively the column densities and ionization fractions of elements a and b in ion states i and j . If the gas is in photoionization equilibrium and optically thin at all far-UV continuum wavelengths, the correction factors, $f(b_j)/f(a_i)$, depend only on the shape of the ionizing spectrum and the ionization parameter U (defined as the dimensionless ratio of the gas to hydrogen-ionizing photon densities at the illuminated face of the cloud).

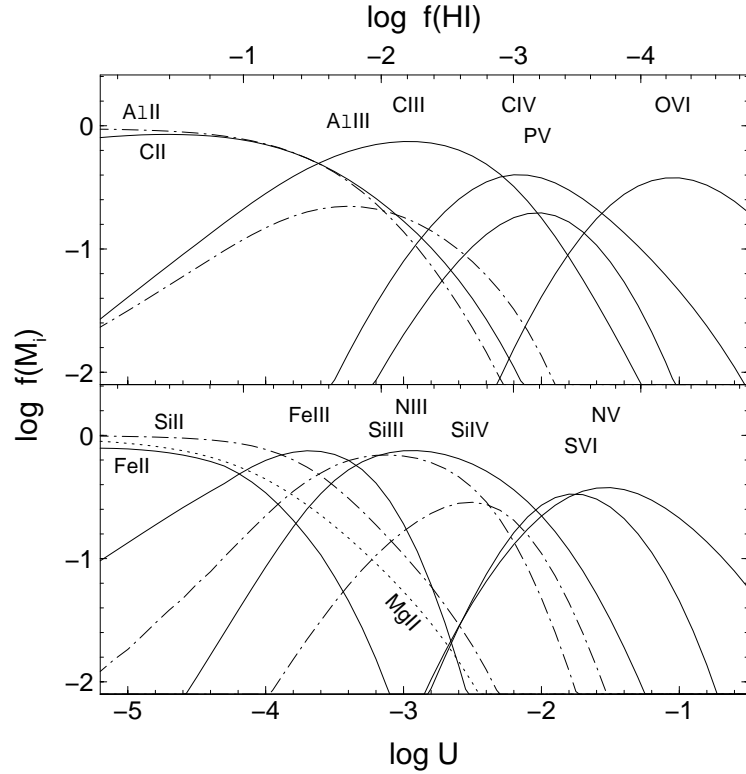


Figure 6. Ionization fractions in optically thin clouds photoionized at different U by a power-law spectrum with index $\alpha = -1.5$. The HI fraction appears across the top. The curves for the metal ions M_i are labeled at their peaks whenever possible. The notation here is SiII = Si^{+2} , etc.

Figure 6 shows theoretical ionization fractions, $f(M_i)$, for various metals, M , in ion stage, i , as a function of the ionization parameter, U , in optically thin photoionized clouds (from HF99). The HI fraction, $f(\text{HI})$, is shown across the top of the figure. The calculations were performed using CLOUDY (version 90.04, Ferland *et al.* 1998) with a power-law ionizing spectrum with index $\alpha = -1.5$, where $f_\nu \propto \nu^\alpha$. Note that the results in Figure 6 are not sensitive to

the specific densities or abundances used in the calculations (within reasonable limits, see Hamann 1997). Ideally, we would constrain the ionization state (i.e. U) in Figure 6 by comparing the column densities in different ionization stages of the same element. We can also constrain the ionization by comparing ions of different metals with some reasonable assumption about their relative abundance. With U thus constrained, Figure 6 provides the correction factors needed to derive abundance ratios from Eqn. 1. Repeating this procedure with calculations for different ionizing spectral shapes yields estimates of the theoretical uncertainties (Hamann 1997).

If the data provide no useful constraints on U (because too few lines are measured) or multiple constraints imply a range of ionization states (as in the $z_a \approx z_e$ system of UM 675, Hamann *et al.* 1995b), we can still derive conservatively low values of $f(\text{HI})/f(\text{M}_i)$ and thus $[\text{M}/\text{H}]$ by assuming each metal line forms where that ion is most abundant (i.e. at the peak of its $f(\text{M}_i)$ curve in Figure 6). We can also place firm lower limits on the $[\text{M}/\text{H}]$ ratios by adopting the minimum correction factor for each M_i . (Every $f(\text{HI})/f(\text{M}_i)$ ratio has a well-defined minimum at U values near the peak in the $f(\text{M}_i)$ curve.) Hamann (1997) presented numerous plots of the minimum and conservatively small ionization corrections for a wide range of ionizing spectral shapes. Note that the correction factors for some important metal-to-metal ion ratios, such as FeII/MgII and PV/CIV, also have well-defined minima that are useful for abundance constraints (see also HF99 and Hamann *et al.* 1999).

5.3. Abundance Results

Table 1 shows the results of applying this analysis to two bona fide intrinsic absorbers, namely, the $z_a \approx z_e$ NALs in UM 675 (Hamann 1997; Hamann *et al.* 1997b) and the BALs in PG 1254+047 (Hamann 1998). The ionic column densities listed for both sources follow from direct integration of the apparent optical depths in the absorption line troughs (see §5.4 below). For UM 675, I adjusted the optical depths for a 50% coverage fraction in all of the metal ions and 100% coverage in HI. These adjustments do not change the derived HI column density, but the columns in the metal ions are roughly doubled. Note that the relatively low column densities in both systems (and the lack of a significant HI Lyman edge in UM 675) support the assumption of low continuum optical depths in the calculations above (Hamann 1997).

The ionization states in both cases are uncertain, so the table lists the conservatively low metal-to-hydrogen ratios, $[\text{M}/\text{H}]_p$, assuming each metal line forms at the peak in its $f(\text{M}_i)$ curve. The table also lists the firm lower limits, $[\text{M}/\text{H}]_{min}$, derived from the minimum correction factors in Hamann (1997). The uncertainties in the table indicate the range of values derived for a reasonable range of ionizing continuum shapes. Keep in mind that these M/H estimates are limiting values that need not agree between ions. The $[\text{M}/\text{H}]$ quantities are typically higher (and more realistic) for the low-ionization metals because the HI lines tend to form with these ions. The $[\text{M}/\text{H}]_p$ results provide our best guess at the actual abundances in UM 675; the overall metallicity is roughly twice solar ($Z \approx 2 Z_\odot$) based on $[\text{C}/\text{H}]$, with nitrogen several times more enhanced. The result for $Z \gtrsim Z_\odot$ is typical of $z_a \approx z_e$ NALs and occurs without exception in the intrinsic systems (Petitjean, Rauch & Carswell 1994, Wampler *et al.* 1993, Tripp

et al. 1996 and 1997, Savage & Tripp 1998, Hamann 1997, Hamann *et al.* 1997c). The NALs thus support the independent evidence from BELs for $Z \gtrsim Z_{\odot}$ and enhanced nitrogen (§4 above).

Table 1. Example Column Densities and Abundances

Ion	$\log N(M_i)$	$[M/H]_p$	$[M/H]_{min}$
UM 675 ($z_a \approx z_e \approx 2.15$)			
H I	14.8	—	—
C III	14.1	$+0.4^{+0.5}_{-0.2}$	$-0.2^{+0.7}_{-0.2}$
C IV	14.9	$+0.4^{+0.7}_{-0.3}$	$-0.1^{+0.9}_{-0.3}$
N III	14.5	$+1.3^{+0.5}_{-0.2}$	$+0.7^{+0.7}_{-0.3}$
N V	15.1	$+0.3^{+0.8}_{-0.4}$	$-0.2^{+0.9}_{-0.3}$
O VI	15.5	$-0.9^{+0.8}_{-0.3}$	$-1.4^{+0.8}_{-0.3}$
Ne VIII	15.7	$-1.1^{+0.7}_{-0.4}$	$-1.4^{+0.7}_{-0.4}$
PG 1254+047 (BAL, $z_e = 1.0$)			
H I	$\lesssim 15.0$	—	—
C IV	15.9	$+1.4^{+0.7}_{-0.4}$	$+1.0^{+0.8}_{-0.4}$
N V	16.2	$+1.4^{+0.8}_{-0.4}$	$+1.0^{+0.8}_{-0.4}$
Si IV	15.0	$+2.0^{+0.6}_{-0.4}$	$+1.8^{+0.6}_{-0.4}$
P V	15.0	$+3.3^{+0.6}_{-0.4}$	$+3.1^{+0.6}_{-0.4}$

The derived BAL column densities lead to much more extreme abundances, with $[\text{Si}/\text{H}] \gtrsim 1.8$ and $[\text{P}/\text{C}] \gtrsim +2.2$ in PG 1254+047. These results are roughly typical of BALs (Turnshek 1988, Turnshek *et al.* 1996, Korista *et al.* 1996, Junkkarinen *et al.* 1997, Hamann 1997). They are too extreme to be compatible with well-mixed interstellar gas enriched by normal stellar populations. Shields (1996) noted that the BAL estimates are similar to the abundances measured in novae. He proposed that novae might dominate the enrichment of BAL regions if the nova rates are enhanced by white dwarfs gaining mass as they plunge through the QSO accretion disk. However, this unusual mechanism is not needed because there appear to be serious problems with the BAL column densities.

5.4. Problems with the BALs

Absorption line optical depths and column densities are derived from the observed intensities, I_{ν} , by the relation, $I_{\nu} = I_o \exp(-\tau_{\nu})$, where I_o is the unabsorbed (continuum) intensity and τ_{ν} is the optical depth at frequency ν (Junkkarinen *et al.* 1983, Grillmair & Turnshek 1987, Korista *et al.* 1992, Savage & Sembach 1991, Jenkins 1996, Arav *et al.* 1999). Partial coverage of the background light source(s) can fill in the troughs and thus lead to underestimated optical depths and column densities. A critical difference between BALs and NALs is in our ability to resolve adjacent multiplet lines and thereby directly measure any partial coverage effects (see Hamann *et al.* 1997b and HF99). In general, this type of analysis is possible for only the NALs, where resolved doublets like CIV $\lambda\lambda 1548, 1550$ or SiIV $\lambda\lambda 1394, 1403$ are easily measurable. The blending of these features in BALs has generally made the partial-coverage analysis impossible.

Hamann (1998) used explicit calculations of the line optical depths to show that BAL spectra are consistent with much lower (solar) metallicities and solar relative abundances if at least the stronger transitions (such as CIV $\lambda 1549$) are more optically thick than they appear. In particular, those calculations suggest that the anomalously large ratio of PV $\lambda 1121$ /CIV $\lambda 1549$ absorption lines results from severe saturation in CIV rather than extreme P/C abundances. The line saturation is disguised in the observed (modest) BAL troughs by partial line-of-sight coverage of the background light source(s).

Arav *et al.* (1999) provided direct evidence for partial coverage in one BAL system based on some far-UV lines (whose true optical depth ratios are fixed by atomic physics). Similar evidence has come from a few BALs or BAL components where the profiles are narrow enough to resolve multiplet transitions that are close in wavelength (Telfer *et al.* 1998, Wampler *et al.* 1995). More indirect evidence for partial coverage in BALs has come from spectropolarimetry (Cohen *et al.* 1995, Goodrich & Miller 1995, Hines & Wills 1995). It is also interesting that the only known NAL system with PV absorption (Barlow *et al.* 1999) has resolved doublet ratios in CIV, SiIV and NV that require severe line saturation and partial line-of-sight coverage.

It is therefore likely that the column densities derived so far from BALs are generally underestimated and the abundances are generally incorrect. Future studies that involve relatively narrow BALs (Telfer *et al.* 1998) or the plethora of hard-to-measure far-UV lines (Arav *et al.* 1999) might yet allow the needed partial-coverage analysis and thus provide reliable abundance estimates.

6. Metallicities and the Baldwin Effect

The “Baldwin Effect” is an empirical trend for decreasing line equivalent widths with increasing luminosity (Baldwin 1977, Kinney *et al.* 1990, Osmer & Shields this volume). Calculations by HF93a showed that most of the line equivalent widths will decline naturally with increasing metallicities (because of the declining gas temperatures, see also HF99). If Z is correlated with the luminosities of QSOs, as suggested by the emission line data (§4.2), then metallicity difference would at least contribute to the Baldwin Effect. An important test of the influence of metallicity will come from the nitrogen lines, because they should run counter to the trend and get relatively stronger with Z (and L) due to the selective N enhancement (§2.4 and §3). Recent observations support this prediction, showing that while CIV and other lines decline with L – the usual Baldwin effect – NV does not (Osmer *et al.* 1994; Laor *et al.* 1995, Korista *et al.* 1998). See Korista *et al.* (this volume) for further discussion.

7. Summary and Future Prospects

In spite of the null results from BALs, there is a growing consensus from the BELs and intrinsic NALs for typically solar or higher metallicities in high-redshift QSOs. These results support models of galaxy evolution wherein vigorous star formation in galactic nuclei (or dense proto-galactic condensations) produces $Z \gtrsim Z_{\odot}$ in the gas at redshifts $z \gtrsim 4$. It is interesting to note that the high metal abundances in dense quasar environments sharply contrast with the

metallicities measured elsewhere at high redshifts. For example, the damped-Ly α absorbers in QSO spectra, which apparently probe lines of sight through intervening disk galaxies (Prochaska & Wolfe 1998 and refs. therein), have mean (gas-phase) metallicities of order $0.05 Z_{\odot}$ at $z \sim 2-3$ (Lu *et al.* 1996, Pettini *et al.* 1997, Lu, Sargent & Barlow 1998). The Ly α forest systems, which presumably probe more extended and tenuous inter-galactic structures (Rauch 1998), typically have metallicities $<0.01 Z_{\odot}$ at high redshifts (Rauch, Haehnelt & Steinmetz 1997, Songalia & Cowie 1996). The much higher metal abundances near QSOs are consistent with the rapid and more extensive evolution expected in dense environments (Gnedin & Ostriker 1997).

These are exciting times for quasar abundance work. The results so far have only scratched the surface of what is possible. The new generations of large ground-based and space-based telescopes are or will soon make it possible to greatly extend the results discussed above. In particular, we will be able to 1) measure a wider variety of both emission and absorption diagnostics and 2) compare the derived abundances in large QSO samples that span a wide range of redshifts and luminosities. The new data will thereby test further the reliability of each diagnostic, search more definitively for trends with redshift or luminosity, examine the range of QSO abundances at any given z or L , and make better measurements of specific evolution probes like the Fe/ α clock. It will be particularly interesting to compare emission and absorption diagnostics in the same objects. For example, one goal should be to test the BEL result for high Fe/Mg abundances by observing FeII/MgII or perhaps FeII/SiIII in NAL systems.

Inevitably, these studies will also improve our general understanding of observational trends between QSO luminosities and the BEL spectra. Abundance variations might be an important ingredient in calibrating the Baldwin Effect for tests of cosmology (§6, also Korista *et al.* this volume).

Acknowledgments. I am grateful to my close collaborators, T. Barlow, F. Chaffee, G. Ferland, C. Foltz, V. Junkkarinen, K. Korista and J. Shields, for their contributions to this work. I also acknowledge support from the Space Telescope Guest Observer program and from NASA through grant NAG 5-3234.

References

- Arav, N., Korista, K.T., de Kool, M., Junkkarinen, V.T., Begelman, M.C. 1999, ApJ, in press
- Aretxaga, I., Terlevich, R.J., & Boyle, B.J. 1998, MNRAS, 296, 643
- Arimoto, N., & Yoshii, Y. 1987, A&A, 173, 23
- Bahcall J.N., Kirhakos S., Saxe D.H., Schneider D.P. 1997, ApJ, 479, 642
- Baldwin, J. 1977, ApJ, 214, 679
- Baldwin, J.A., Ferland, G.J., Korista, K.T., Verner, D. 1995, ApJ, 455, L119
- Baldwin, J.A., & Netzer, H. 1978, ApJ, 226, 1
- Barlow, T. A. *et al.* 1999, in prep.
- Barlow, T. A., & Junkkarinen, V. T. 1994, BAAS, 26, 1339
- Barlow, T. A., & Sargent, W. L. W. 1997, AJ, 113, 136

- Bender, R., Burstein, D., & Faber, S.M. 1993, ApJ, 411, 153
- Bica, E., Alloin, D., & Schmidt, A.A. 1990, A&A, 228, 23
- Bica, E., Arimoto, N., & Alloin, D. 1988, A&A, 202, 8
- Boyle B. 1990, MNRAS, 243, 231
- Bruzual, G., Barbuy, B., Ortolani, S., Bica, E., & Cuisinier, F. 1997, AJ, 114, 1531
- Carroll, S. M., Press, W. H. 1992, ARAA, 30, 499
- Cohen, M.H., Ogle, P.M., Tran, H.D., Vermeulen, R.C., Miller, J.S., *et al.* 1995, ApJ, 448, L77
- Connolly, A. A., Szalay, A. S., Dickenson, M., SubbaRao, M. U., & Brunner, R. J. 1997, ApJ, 486, L11
- Davidson, K., & Netzer, H. 1979, Rev. Mod. Phys., 51, 715
- Faber, S.M. 1973, ApJ, 179, 423
- Ferland, G. J., Baldwin, J. A., Korista, K. T., Hamann, F., Carswell, R. F., Phillips, M., Wilkes, B., & Williams, R. E. 1996, ApJ, 461, 683
- Ferland, G.J., Korista, K.T., Verner, D.A., Ferguson, J.W., Kingdon, J.B., *et al.* 1998, PASP, 110, 761
- Ferland, G. J., Peterson, B. M., Horne, K., Welsch, W. F., & Nahar, S. N. 1992, ApJ, 387, 95
- Geisler, D., & Friel, D.E. 1992, AJ, 104, 128
- Gnedin, N.Y., & Ostriker, J.P. 1997, ApJ, 486, 581
- Goodrich, R. W., & Miller, J. S. 1995, ApJ, 448, L73
- Gorgas, J., Efstathiou, G., Aragón Salamanca, A.A. 1990, MNRAS, 245, 217
- Green, P. J., & Mathur, S. 1996, ApJ, 462, 637
- Grillmair, C.J., & Turnshek, D.A. 1987, in QSO Absorption Lines: Probing the Universe, Poster Papers, eds. J.C. Blades, C. Norman, D.A. Turnshek, p. 1
- Haehnelt, M.G., Natarajan, P., & Rees, M.J. 1998, MNRAS, 300, 817
- Haehnelt, M.G., & Rees, M.J. 1993, MNRAS, 263, 168
- Haiman, Z., & Loeb, A. 1998, ApJ, 503, 505
- Hamann, F. 1997, ApJS, 109, 279
- Hamann, F. 1998, ApJ, 500, 798
- Hamann, F., Barlow, T. A., Beaver, E. A., Burbidge, E. M., Cohen, R. D., Junkkarinen, V., & Lyons, R. 1995b, ApJ, 443, 606
- Hamann, F., Barlow, T.A., Cohen, R.D., Junkkarinen, V., Burbidge, E.M. 1997c, in Mass Ejection From AGN, eds. R. Weymann, I. Shlosman, N. Arav, ASP Conf. Series, 128, 187
- Hamann, F., Barlow, T. A., Junkkarinen, V., & Burbidge, E. M., 1997b, ApJ, 478, 80
- Hamann, F., Cohen, R. D., Shields, J. C., Burbidge, E. M., Junkkarinen, V., & D. M. Crenshaw 1998, ApJ, 496, 761
- Hamann, F., & Ferland, G. J. 1992, ApJL, 391, L53
- Hamann, F., & Ferland, G. J. 1993a, ApJ, 418, 11 (HF93a)

- Hamann, F., & Ferland, G. J. 1999, ARAA, 37, xx (HF99)
- Hamann, F., & Ferland, G. J. 1993b. Rev. Mex. Astr. Astrof., 26, 53
- Hamann, F., & Korista, K. T. 1996, ApJ, 464, 158
- Hamann, F., Korista, K.T., & Ferland, G. J. 1999, in prep.
- Hamann, F., Shields, J.C., Cohen, R.D., Junkkarinen, V.T., Burbidge, E.M. 1997a, in Emission Lines From Active Galaxies: New Methods and Techniques, IAU Col. 159, eds. B.M. Peterson, F.-Z. Cheng, A.S. Wilson, ASP Conf. Ser., 113, 96
- Hamann, F., Shields, J. C., Ferland, G. J., & Korista, K. T. 1995a, ApJ, 454, 688
- Hines, D. C., & Wills, B. J. 1995, ApJ, 448, L69
- Idiart, T.P., De Freitas Pacheco, J.A., & Costa, R.D.D. 1996, AJ, 112, 2541
- Isotov, Y.I., Thuan, T.X. 1999, ApJ, in press
- Jenkins, E.B. 1996, ApJ, 471, 292
- Junkkarinen, V.T., Burbidge, E.M., & Smith, H.E. 1983, ApJ, 265, 51
- Junkkarinen, V. T., *et al.* 1997, in Mass Ejection From AGN, eds. R. Weymann, I. Shlosman, and N. Arav, ASP Conf. Series, 128, 220
- Kinney, A.L., Rivolo, A.R., & Koratkar, A.R. 1990, ApJ, 357, 338
- Köppen, J., & Arimoto, N. 1990, A&A, 240, 22
- Korista, K. T., Baldwin, J. & Ferland, G. J., 1998, ApJ, 507, 24
- Korista, K. T., Hamann, F., Ferguson, J., & Ferland, G. J. 1996, ApJ, 461, 641
- Korista, K. T., Weymann, R. J., Morris, S. L., Kopko Jr., M., Turnshek, D. A., Hartig, G. F., Burbidge, E. M., & Junkkarinen, V. T. 1992, ApJ, 401, 529
- Kormendy, J., Bender, R., Evans, A. S., Richstone, D. 1998, AJ, 115, 1823
- Krolik, J., & Voit, G.M. 1998, ApJ, 497, L5
- Laor, A., Bahcall, J.N., Jannuzi, B.T., Schneider, D.P., Green, R.F. 1995, ApJS, 99, 1
- Larson, R.J. 1974, MNRAS, 169, 229
- Loeb, A., & Rasio, F.A. 1994, ApJ, 432, 52
- Lu, L., Sargent, W. L. W, & Barlow, T. A. 1998, AJ, 115, 55
- Magorrian, J., Tremaine, S., Richstone, D., Bender, R., Bower, G., *et al.* 1998, AJ, 115, 2285
- Mathews, W. G., & Ferland, G. J. 1987, ApJ, 323, 456
- Mathur, S., Elvis, M., & Singh, K. P. 1995, ApJ, 455, L9
- Matteucci, F., & Brocato, E. 1990, ApJ, 365, 539
- Matteucci, F., & Tornambè, A. 1987, A&A, 185, 51
- McLeod, K.K. 1998, in Quasar Hosts, ESO-IAC Conf. Proc., ed. DL Clements, I Pérez-Fouron, (New York:Springer), xx
- McLeod, K.K., & Rieke G.H. 1995, ApJ, 454, L77
- McLure, R. J., Dunlop, J.S., Kukula, M.J., Baum, S.A., O’Dea, C. P., *et al.* 1998, preprint (astro-ph/9809030)
- Miller, J., Tran, H., & Sheinis, A. 1996, BAAS, 28, 1031

- Minniti, D., Olszewski, E.W., Liebert, J., White, S.D., Hill, J.M., *et al.* 1995, MNRAS, 277, 1293
- Osmer, P. S. 1980, ApJ, 237, 666
- Osmer, P. S., Porter, A. C., & Green, R. F. 1994, ApJ, 436, 678
- Osmer, P. S., & Smith, M. G. 1976, ApJ, 210, 267
- Osmer, P. S., & Smith, M. G. 1977, ApJ, 213, 607
- Peterson, B. 1993, PASP, 105, 247
- Petitjean, P., Rauch, M., & Carswell, R. F. 1994, A&A, 291, 29
- Pettini M., King D. L., Smith L. J., & Hunstead R. W. 1997, ApJ, 486, 665
- Prochaska, J.X., & Wolfe, A. M. 1998, ApJ, 507, 113
- Rauch, M. 1998, ARAA, 36, 267
- Rauch, M., Haehnelt, M.G., & Steinmetz, M. 1997, ApJ, 481, 601
- Rich, R. M. 1988, AJ, 95, 828
- Rich, R. M. 1990, ApJ, 362, 604
- Savage, B.D., & Sembach, K.R. 1991, ApJ, 379, 245
- Savage, B.D., Tripp, T.M., & Lu, L. 1998, AJ, 115, 436
- Scalo, J. M. 1990, in Windows on Galaxies, eds. G. Fabbiano, J.S. Gallagher, & A. Renzini (Dordrecht:Kluwer), 125
- Schneider, D. P., Schmidt, M., & Gunn, J. E. 1991, AJ, 101, 2004
- Searle, L., & Zinn, R. 1978, ApJ, 225, 357
- Shields, G. A., 1976, ApJ, 204, 330
- Shields, G. A., 1996, ApJ, 461, L9
- Sigut, T.A.A., & Pradhan, A.K. 1998, ApJ, 499, L139
- Songalia, A., Cowie, L.L. 1996, AJ, 112, 335
- Steidel, C. C., Adelberger K. L., Dickenson, M., Giavalisco, M., Pettini, M., *et al.* 1998, ApJ, 492, 428
- Taniguchi, Y., Arimoto, N., Murayama, T., Evans, A.S., Sanders, D.B., *et al.* 1997, in Quasar Hosts, eds. D.L. Clements, I. Perez-Fouron, ESO-IAC Conf. Pro., 127
- Telfer, R.C., Kriss, G.A., Zheng, W., Davidsen, A.F., Green, R.F. 1999, ApJ, in press
- Thompson, K.L., Elston, R., & Hill, G.J. 1999, preprint
- Tinsley, B. 1980, *Fund. of Cosmic Phys.*, 5, 287
- Tripp, T. M., Lu, L., & Savage, B. D. 1996, ApJS, 102, 239
- Tripp, T. M., Lu, L., & Savage, B. D. 1997, ApJS, 112, 1
- Turner, E.L. 1991, AJ, 101, 5
- Turnshek, D. A. 1988, in QSO Absorption Lines: Probing the Universe, eds. J. C. Blades, D. A. Turnshek, & C. A. Norman (Cambridge: Cambridge Univ. Press), 17
- Turnshek, D.A., Kopko, M., Monier, E., Noll, D., Espey, B., *et al.* 1996, ApJ, 463, 110
- Uomoto, A. 1984, ApJ, 284, 497

- Van Zee, L., Salzer, J. J., & Haynes, M. P. 1998, *ApJ*, 497, L1
- Verner, E.M., Verner, D.A., Korista, K.T., Ferguson, J.W., Hamann, F., *et al.*
1999, *ApJ*, in press
- Véron-Cetty, M. P., Véron, P., & Tarengi, M. 1983, *A&A*, 119, 69
- Vila-Costas, M. B., & Edmunds, M. G. 1993, *MNRAS*, 265, 199
- Wampler, E.J., Bergeron, J., & Petitjean, P. 1993, *AA*, 273, 15
- Wampler, E.J., Chugal, N.N., & Petitjean, P. 1995, *ApJ*, 443, 586
- McWilliam, A., Rich, R.M. 1994, *ApJS*, 91, 749
- Weymann, R. J., *et al.* 1991, *ApJ*, 373, 23
- Wheeler, J.C., Sneden, C., & Truran J.W. 1989, *ARAA*, 27, 279
- Wills, B. J., Netzer, H., & Wills, D. 1985, *ApJ*, 288, 94
- Worthey, G., Faber, S. M., & Jesús Gonzalez, J. 1992, *ApJ*, 398, 69
- Yoshii, Y., Tsujimoto, T., & Nomoto, K. 1996, *ApJ*, 462, 266
- Zaritsky, D., Kennicutt, R.C., & Huchra, J.P. 1994, *ApJ*, 420, 87